

# Tests of Bayesian Model Selection Techniques for Gravitational Wave Astronomy

Neil J. Cornish and Tyson B. Littenberg

*Department of Physics, Montana State University, Bozeman, MT 59717*

The analysis of gravitational wave data involves many model selection problems. The most important example is the detection problem of selecting between the data being consistent with instrument noise alone, or instrument noise and a gravitational wave signal. The analysis of data from ground based gravitational wave detectors is mostly conducted using classical statistics, and methods such as the Neyman-Pearson criteria are used for model selection. Future space based detectors, such as the *Laser Interferometer Space Antenna* (LISA), are expected to produced rich data streams containing the signals from many millions of sources. Determining the number of sources that are resolvable, and the most appropriate description of each source poses a challenging model selection problem that may best be addressed in a Bayesian framework. An important class of LISA sources are the millions of low-mass binary systems within our own galaxy, tens of thousands of which will be detectable. Not only are the number of sources unknown, but so are the number of parameters required to model the waveforms. For example, a significant subset of the resolvable galactic binaries will exhibit orbital frequency evolution, while a smaller number will have measurable eccentricity. In the Bayesian approach to model selection one needs to compute the Bayes factor between competing models. Here we explore various methods for computing Bayes factors in the context of determining which galactic binaries have measurable frequency evolution. The methods explored include a Reverse Jump Markov Chain Monte Carlo (RJMCMC) algorithm, Savage-Dickie density ratios, the Schwarz-Bayes Information Criterion (BIC), and the Laplace approximation to the model evidence. We find good agreement between all of the approaches.

## I. BACKGROUND

Bayesian statistical techniques are becoming increasingly popular in gravitational wave data analysis, and have shown great promise in tackling the various difficulties of gravitational wave (GW) source extraction from modeled data for the Laser Interferometer Space Antenna (LISA). A powerful tool in the suite of Bayesian methods is that of quantitative model selection [1, 2]. To understand why this is a valuable feature consider a scenario where one is attempting to fit data with two competing models of differing dimension. In general, a higher dimensional model will produce a better fit to a given set of data. This can be taken to the limit where there are as many model parameters as there are data points allowing one to perfectly match the data. The problem then is to decide how many parameters are physically meaningful and to select the model containing only those parameters. In the context of GW detection these extra parameters could be additional physical parameters used to model the source or additional sources in the data. If a model is over-parameterized it will over-fit the data and produce spurious results.

Many of the model selection problems associated with LISA astronomy involve *nested* models, where the simpler model forms a subset of the more complicated model. The problem of determining the number of resolvable galactic binaries, and the problem of determining the number of measurable source parameters, are both examples of nested model selection. One could argue that the later is better described as “approximation selection” since we are selecting between different parameterizations of the full 17 dimensional physical model that describes the signals from binary systems of point masses in general

relativity. However, many similar modeling problems in astrophysics and cosmology [2], as well as in other fields such as geophysics [3], are considered to be examples of model selection, and we will adopt that viewpoint here.

The LISA observatory [4] is designed to explore the low frequency portion of the gravitational wave spectrum between  $\sim 0.1 \rightarrow 100$  mHz. This frequency region will be heavily populated by signals from galactic binary systems composed of stellar mass compact objects (e.g. white dwarfs and neutron stars), of which millions are theorized to exist. Tens of thousands of these GW sources will be resolvable by LISA and the remaining sources will contribute to a confusion-limited background [5]. This is expected to be the dominant source of low frequency noise for LISA.

Detection and subsequent regression of the galactic foreground is of vital importance in order to then pursue dimmer sources that would otherwise be buried by the foreground. Because of the great number of galactic sources, and the ensuing overlap between individual sources, a one-by-one detection/regression is inaccurate [6]. Therefore a global fit to all of the galactic sources is required. Because of the uncertainty in the number of resolvable sources one can not fix the model dimension *a priori* which presents a crucial model selection problem. Over-fitting the data will result in an inaccurate regression which would then remove power from other sources in the data-stream, negatively impacting their detection and characterization. The Reverse Jump Markov Chain Monte Carlo approach to Bayesian model selection has been used to determine the number of resolvable sources in the context of a toy problem [7, 8] which shares some of the features of the LISA foreground removal problem. Meanwhile the Laplace approximation to Bayesian

model selection has been employed to estimate the number of resolvable sources as part of a MCMC based algorithm to extracting signals from simulated LISA data streams [6, 9].

Another important problem for GW astronomy is the determination of which parameters need to be included in the description of the waveforms. For example, the GW signal from a binary inspiral, as detected by LISA, may involve as many as 17 parameters. However, for massive black hole binaries of comparable mass we expect the eccentricity to be negligible, reducing the model dimension to 15, while for extreme mass ratio systems we expect the spin of the smaller body to have little impact on the waveforms, reducing the model dimension to 14. In many cases the inspiral signals may be described by even fewer parameters. For low mass galactic binaries spin effects will be negligible (removing six parameters), and various astrophysical processes will have circularized the orbits of the majority of systems (removing two parameters). Of the remaining nine parameters, two describe the frequency evolution - *e.g.* the first and second time derivatives of the GW frequency, which may or may not be detectable [27].

Here we investigate the application of Bayesian model selection to LISA data analysis in the context of determining the conditions under which the first time derivative of the GW frequency,  $\dot{f}$ , can be inferred from the data. We parameterize the signals using the eight parameters

$$\vec{\lambda} \rightarrow (A, f, \theta, \phi, \psi, \iota, \varphi_0, \dot{f}) \quad (1)$$

where  $A$  is the amplitude,  $f$  is the initial gravitational wave frequency,  $\theta$  and  $\phi$  are the ecliptic co-latitude and longitude,  $\psi$  is the polarization angle,  $\iota$  is the orbital inclination of the binary and  $\varphi_0$  is the GW phase. The parameters  $f$ ,  $\dot{f}$  and  $\varphi_0$  are evaluated at some fiducial time (*e.g.* at the time the first data is taken). For our analysis only a single source is injected into the simulated data streams. In the frequency domain the output  $s(f)$  in channel  $\alpha$  can be written as

$$\tilde{s}_\alpha(f) = \tilde{h}_\alpha(\vec{\lambda}) + \tilde{n}_\alpha(f) \quad (2)$$

where  $\tilde{h}_\alpha(\vec{\lambda})$  is the response of the detector to the incident GW and  $\tilde{n}_\alpha(f)$  is the instrument noise. For our work we will assume stationary Gaussian instrument noise with no contribution from a confusion background. In our analysis we use the noise orthogonal  $A, E, T$  data streams, which can be constructed from linear combinations of the Michelson type  $X, Y, Z$  signals:

$$\begin{aligned} A &= \frac{1}{3}(2X - Y - Z), \\ E &= \frac{1}{\sqrt{3}}(Z - Y), \\ T &= \frac{1}{3}(X + Y + Z). \end{aligned} \quad (3)$$

This set of  $A, E, T$  variables differ slightly from those constructed from the Sagnac signals [10]. We do not use

the  $T$  channel in our analysis as it is insensitive to GWs at the frequencies we are considering. The noise spectral density in the  $A, E$  channels has the form

$$\begin{aligned} S_n(f) &= \frac{4}{3}(1 - \cos(2f/f_*)) \left( (2 + \cos(f/f_*))S_s \right. \\ &\quad \left. + 2(3 + 2\cos(f/f_*) + \cos(2f/f_*))S_a \right) \text{Hz}^{-1} \end{aligned} \quad (4)$$

where  $f_* = 1/2\pi L$ , and the acceleration noise  $S_a$  and shot noise  $S_s$  are simulated at the levels

$$\begin{aligned} S_a &= \frac{10^{-22}}{L^2} \text{Hz}^{-1} \\ S_s &= \frac{9 \times 10^{-30}}{(2\pi f)^4 L^2} \text{Hz}^{-1}. \end{aligned} \quad (5)$$

Here  $L$  is the LISA arm length ( $\approx 5 \times 10^9$  m).

Of central importance to Bayesian analysis is the posterior distribution function (PDF) of the model parameters. The PDF  $p(\vec{\lambda}|s)$  describes the probability that the source is described by parameters  $\vec{\lambda}$  given the signal  $s$ . According to Bayes' Theorem,

$$p(\vec{\lambda}|s) = \frac{p(\vec{\lambda})p(s|\vec{\lambda})}{\int d\vec{\lambda} p(\vec{\lambda})p(s|\vec{\lambda})} \quad (6)$$

where  $p(\vec{\lambda})$  is the *a priori*, or prior, distribution of the parameters  $\vec{\lambda}$  and  $p(s|\vec{\lambda})$  is the likelihood that we measure the signal  $s$  if the source is described by the parameters  $\vec{\lambda}$ . We define the likelihood using the noise weighted inner product

$$(A|B) \equiv \frac{2}{T} \sum_\alpha \sum_f \frac{\tilde{A}_\alpha^*(f)\tilde{B}_\alpha(f) + \tilde{A}_\alpha(f)\tilde{B}_\alpha^*(f)}{S_n^\alpha(f)} \quad (7)$$

as

$$p(s|\vec{\lambda}) = C \exp \left[ -\frac{1}{2} \left( s - h(\vec{\lambda}) \middle| s - h(\vec{\lambda}) \right) \right] \quad (8)$$

where the normalization constant  $C$  depends on the noise, but not the GW signal. One goal of the data analysis method is to find the parameters  $\vec{\lambda}$  which maximizes the posterior. Markov Chain Monte Carlo (MCMC) methods are ideal for this type of application [11]. The MCMC algorithm will simultaneously find the parameters which maximize the posterior and accurately map out the PDF of the parameters. This is achieved through the use of a Metropolis-Hastings [12, 13] exploration of the parameter space. A brief description of this process is as follows: The chain begins at some random position  $\vec{x}$  in the parameter space and subsequent steps are made by randomly proposing a new position in the parameter space  $\vec{y}$ . This new position is determined by drawing from some proposal distribution  $q(\vec{x}|\vec{y})$ . The choice of whether or not adopt the new position  $\vec{y}$  is made by calculating the Hastings ratio (transition probability)

$$\alpha = \min \left\{ 1, \frac{p(\vec{y})p(s|\vec{y})q(\vec{y}|\vec{x})}{p(\vec{x})p(s|\vec{x})q(\vec{x}|\vec{y})} \right\} \quad (9)$$

and comparing  $\alpha$  to a random number  $\beta$  taken from a uniform draw in the interval  $[0:1]$ . If  $\alpha$  exceeds  $\beta$  then the chain adopts  $\vec{y}$  as the new position. This process is repeated until some convergence criterion is satisfied. The MCMC differs from a Metropolis extremization by forbidding proposal distributions that depend on the past history of the chain. This ensures that the progress of the chain is Markovian and therefore statistically unbiased. Once the chain has stabilized in the neighborhood of the best fit parameters all previous steps of the chain are excluded from the statistical analysis (these early steps are referred to as the “burn in” phase of the chain) and henceforth the number of iterations the chain spends at different parameter values can be used to infer the PDF.

The power of the MCMC is two-fold: Because the algorithm has a finite probability of moving away from a favorable location in the parameter space it can avoid getting trapped by local features of the likelihood surface. Meanwhile, the absence of any “memory” within the chain of past parameter values allows the algorithm to blindly, statistically, explore the region in the neighborhood of the global maximum. It is then rigorously proven that an MCMC will (eventually) perfectly map out the PDF, completely removing the need for user input to determine parameter uncertainties or thresholds.

The parameter vector that maximizes the posterior distribution is stored as the maximum *a posteriori* (MAP) value and is considered to be the best estimate of the source parameters. Note that because of the prior weighting in the definition of the PDF this is not necessarily the  $\vec{\lambda}$  that yields the greatest likelihood. Upon obtaining the MAP value for a particular model  $X$  the PDF, now written as  $p(\vec{\lambda}, X|s)$ , can be employed to solve the model selection problem.

## II. BAYES FACTOR ESTIMATES

The Bayes Factor  $B_{XY}$  [14] is a comparison of the *evidence* for two competing models,  $X$  and  $Y$ , where

$$p_X(s) = \int d\vec{\lambda} p(\vec{\lambda}, X|s) \quad (10)$$

is the marginal likelihood, or evidence, for model  $X$ . The Bayes Factor can then be calculated by

$$B_{XY}(s) = \frac{p_X(s)}{p_Y(s)}. \quad (11)$$

The Bayes Factor has been described as the Holy Grail of model selection: It is a powerful entity that is very difficult to find. The quantity  $B_{XY}$  can be thought of as the odds ratio for a preference of model  $X$  over model  $Y$ . Apart from carefully concocted toy problems, direct calculation of the evidence, and therefore  $B_{XY}$ , is impractical. To determine  $B_{XY}$  the integral required to compute  $p_X$  can not generally be solved analytically and for high dimension models Monte-Carlo integration proves

$B_{XY}$	$2 \log B_{XY}$	Evidence for model $X$
$< 1$	$< 0$	Negative (supports model $Y$ )
1 to 3	0 to 2	Not worth more than a bare mention
3 to 12	2 to 5	Positive
12 to 150	5 to 10	Strong
$> 150$	$> 10$	Very Strong

TABLE I:  $B_{XY}$  ‘confidence’ levels taken from [1]

to be inefficient. To employ this powerful statistical tool various estimates for the Bayes Factor have been developed that have different levels of accuracy and computational cost [1, 2]. We have chosen to focus on four such methods: Reverse Jump Markov Chain Monte Carlo and Savage-Dickie density ratios, which directly estimate the Bayes factor, and the Schwarz-Bayes Information Criterion (BIC) and Laplace approximations of the model evidence.

### A. RJMCMC

Reverse Jump Markov Chain Monte Carlo (RJMCMC) algorithms are a class of MCMC algorithms which admit “trans-dimensional” moves between models of different dimension [3, 15, 16]. For the trans-dimensional implementation applicable to the LISA data analysis problem the choice of model parameters becomes one of the search parameters. The algorithm proposes parameter ‘birth’ or ‘death’ moves (proposing to include or discard the ‘extra’ parameter(s)) while holding all other parameters fixed. The priors in the RJMCMC Hastings ratio

$$\alpha = \min \left\{ 1, \frac{p(\vec{\lambda}_Y)p(s|\vec{\lambda}_Y)g(\vec{u}_Y)}{p(\vec{\lambda}_X)p(s|\vec{\lambda}_X)g(\vec{u}_X)} |\mathbf{J}| \right\} \quad (12)$$

automatically penalizes the posterior density of the higher dimensional model, which compensate for its generically higher likelihood, serving as a built in ‘Occam Factor.’ The  $g(\vec{u})$  which appears in (12) is the distribution from which the random numbers  $\vec{u}$  are drawn and  $|\mathbf{J}|$  is the Jacobian

$$|\mathbf{J}| \equiv \left| \frac{\partial(\vec{\lambda}_Y, \vec{u}_Y)}{\partial(\vec{\lambda}_X, \vec{u}_X)} \right| \quad (13)$$

The chain will tend to spend more iterations using the model most appropriately describing the data, making the decision of which model to favor a trivial one. To quantitatively determine the Bayes Factor one simply computes the ratio of the iterations spent within each model.

$$B_{XY} \simeq \frac{\# \text{ of iterations in model } X}{\# \text{ of iterations in model } Y} \quad (14)$$

Like the simpler MCMC methods, the RJMCMC is *guaranteed* to converge on the correct value of  $B_{XY}$  making

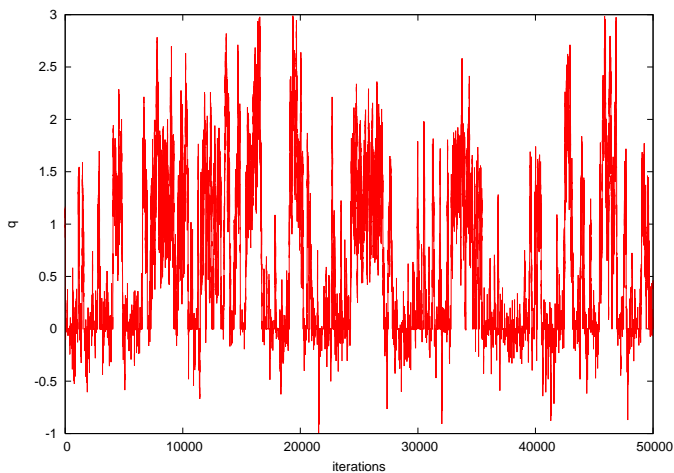


FIG. 1: 50 000 iteration segment of an RJMCMC chain moving between models with and without frequency evolution. This particular run was for a source with  $q = 1$  and  $\text{SNR}=10$  and yielded  $B_{XY} \sim 1$ .

it the ‘gold standard’ of Bayes Factor estimation. And, like regular MCMCs, the convergence can be very slow, so that in practice the Bayes Factor estimates can be inaccurate. This is especially true when the trans-dimensional moves involve many parameters, such as the 7 or 8 dimensional jumps that are required to transition between models with differing numbers of galactic binaries.

Figure 1 shows the output of a RJMCMC search of a simulated LISA data stream containing the signal from a galactic binary with  $q = \dot{f}T_{\text{obs}}^2 = 1$  and an observation time of  $T_{\text{obs}} = 2$  years. The chain moved freely between the 7-dimensional model with no frequency evolution and the 8-dimensional model which included the frequency evolution.

## B. Laplace Approximation

A common approach to model selection is to approximate the model evidence directly. Working under the assumption that the PDF is Gaussian, the integral in equation (10) can be estimated by use of the Laplace approximation. This is accomplished by comparing the volume of the models parameter space  $V$  to that of the parameter uncertainty ellipsoid  $\Delta V$

$$p_X(s) \simeq p(\vec{\lambda}_{\text{MAP}}, X|s) \left( \frac{\Delta V_X}{V_X} \right). \quad (15)$$

The uncertainty ellipsoid can be determined by calculating the determinant of the Hessian  $\mathcal{H}$  of partial derivatives of the posterior with respect to the model parameter evaluated at the MAP value for the parameters.

$$p_X(s) \simeq p(\vec{\lambda}_{\text{MAP}}, X|s) \frac{(2\pi)^{D/2}}{\sqrt{\det \mathcal{H}}} \quad (16)$$

The Fisher Information Matrix (FIM)  $\mathbf{\Gamma}$  with components

$$\Gamma_{ij} \equiv (h_{,i} | h_{,j}) \quad \text{where } h_{,i} \equiv \frac{\partial h}{\partial \lambda^i} \quad (17)$$

can be used as a quadratic approximation to  $\mathcal{H}$  yielding

$$p_X(s) \simeq p(\vec{\lambda}_{\text{MAP}}, X|s) \frac{(2\pi)^{D/2}}{\sqrt{\det \mathbf{\Gamma}}} \quad (18)$$

We will refer to this estimate of the evidence as the Laplace-Fisher (LF) approximation. The LF approximation breaks down if the priors have large gradients in the vicinity of the MAP parameter estimates. The FIM estimates can also be poor if some of the source parameters are highly correlated, or if the quadratic approximation fails. In addition, the FIM approximation gets progressively worse as the SNR of the source decreases.

A more accurate (though more costly) method for estimating the evidence is the Laplace-Metropolis (LM) approximation which employs the PDF as mapped out by the MCMC exploration of the likelihood surface to estimate  $\mathcal{H}$  [16]. This can be accomplished by fitting a minimum volume ellipsoid (MVE) to the  $D$ -dimensional posterior distribution function. The principle axes of the MVE lie in eigen-directions of the distribution which generally do not lie along the parameter directions. Here we employ the `MVE.jar` package which utilizes a genetic algorithm to determine the MVE of the distribution and returns the covariance matrix of the PDF [17]. The determinant of the covariance matrix can then be used to determine the evidence via

$$p_X(s) \simeq p(\vec{\lambda}_{\text{MAP}}, X|s) (2\pi)^{D/2} \sqrt{\det \mathbf{C}}. \quad (19)$$

In the MCMC literature the LM approximation is generally considered to be second only to the RJMCMC method for estimating Bayes Factors.

## C. Savage Dickie Density Ratio

Both RJMCMC and LM require exploration of the posterior for each model under consideration. The Savage-Dickie (SD) approximation estimates the Bayes Factor directly while only requiring exploration of the highest dimensional space [2, 18]. This approximation requires that two conditions are met: Model X must be nested within Model Y (adding and subtracting parameters clearly satisfies this condition) and the priors for any given model must be separable (i.e.  $p(\vec{\lambda}) = p(\lambda^1) \times p(\lambda^2) \times \dots \times p(\lambda^D)$ ) which is, to a good approximation, satisfied in our example. The Bayes Factor  $B_{XY}$  is then calculated by comparing the weight of the marginalized posterior to the weight of the prior distribution for the ‘extra’ parameter at the default, lower-dimensional, value for the parameter in question.

$$B_{XY}(s) \simeq \frac{p(\lambda_0|s)}{p(\lambda_0)} \quad (20)$$

It is interesting to note that if the above conditions are precisely satisfied it can then be shown that this is an exact calculation of  $B_{XY}$  (assuming sufficient sampling of the PDF), as opposed to an approximation.

#### D. Schwarz-Bayes Information Criterion

All of the approximations discussed so far depend on the supplied priors  $p(\vec{\lambda})$ . The Schwarz-Bayes Information Criterion (BIC) method is an approximation to the model evidence which makes its own assumptions about the priors - namely that they take the form of a multivariate Gaussian with covariance matrix derived from the Hessian  $\mathcal{H}$  [16, 19]. The BIC estimate for the evidence is then

$$\ln p_X(s) \simeq \ln p(\vec{\lambda}_{\text{MAP}}, X|s) - \frac{D_X}{2} \ln N_{\text{eff}} \quad (21)$$

where  $D_X$  is the dimension of model  $X$  and  $N_{\text{eff}}$  is the *effective* number of samples in the data. For our tests we defined  $N_{\text{eff}}$  to be the number of data points required to return a (power) signal-to-noise ratio of  $\text{SNR}^2 - D$ , where SNR is the signal-to-noise one gets by summing over the entire LISA band. This choice was motivated by the fact that the variance in  $\text{SNR}^2$  is equal to  $D^2$ , so  $N_{\text{eff}}$  accounts for the data points that carry significant weight in the model fit. The BIC estimate has the advantage of being very easy to calculate, but is generally considered less reliable than the other techniques we are using.

### III. CASE STUDY

To compare the various approximations to the Bayes Factor we simulated a ‘typical’ galactic binary. The injected parameters for our test source can be found in table II. Since  $\dot{f} \sim f^{11/3}$ , higher frequency sources are more likely to have a measurable  $\dot{f}$ . On the other hand, the number of binaries per frequency bin falls off as  $\sim f^{-11/3}$ , so high frequency systems are fairly rare. As a compromise, we selected a system with a GW frequency of 5 mHz. To describe the frequency evolution we introduced the dimensionless parameter

$$q \equiv \dot{f} T_{\text{obs}}^2, \quad (22)$$

which measures the change in the Barycenter GW frequency in units of  $1/T_{\text{obs}}$  frequency bins. For  $q \gg 1$  it is reasonable to believe that a search algorithm will have no difficulty detecting the frequency shift. Likewise, for  $q \ll 1$  it is unlikely that the frequency evolution can be detected (at least for sources with modest SNR). Therefore we have selected  $q \sim 1$  to test the model selection techniques. Achieving  $q = 1$  for typical galactic binaries at 5 mHz requires observation times of approximately two years. A range of SNRs were explored by varying the distance to the source.

TABLE II: Source parameters

$f$ (mHz)	$\cos \theta$	$\phi$ (deg)	$\psi$ (deg)	$\cos \iota$	$\varphi_0$ (deg)	$q$	$T_{\text{obs}}$ (yr)
5.0	1.0	266.0	51.25	0.17	204.94	1	2

We can rapidly calculate accurate waveform templates using the fast-slow decomposition described in the Appendix. Our waveform algorithm has been used in the second round of Mock LISA Data Challenges [20] to simulate the response to a galaxy containing some 26 million sources. The simulation takes just a few hours to run on a single 2 GHz processor.

We simulated a 1024 frequency bin snippet of LISA data around 5 mHz that included the injected signal and stationary Gaussian instrument noise. The Markov chains were initialized at the injected source parameters as the focus of this study is the statistical character of the detection, and not the initial detection (a highly efficient solution to the detection problem is described in Ref. [9]). We used uniform priors for all of the parameters, with the angular parameters taking their standard ranges. We took the frequency to lie somewhere within the frequency snippet, and  $\ln A$  to be uniform across the range  $\frac{1}{2} \ln(S_n/(2T))$  and  $\frac{1}{2} \ln(1000S_n/(2T))$ , which roughly corresponds to signal SNRs in the range 1 to 1000. We took the frequency evolution parameter  $q$  to be uniformly distributed between -3 and 3 and adopted  $q = 0$  as the default value when operating under the 7-dimensional model. In reality, astrophysical considerations yield a very strong prior for  $q$  (see Section V) that will significantly impact model selection. We decided to use a simple uniform prior to compare the various approximations to the Bayes Factor, before moving on to consider the effects of the astrophysical prior in Section V.

The choice of proposal distribution  $q(\vec{x}|\vec{y})$  from which to draw new parameter values has no effect on the asymptotic form of the recovered PDFs, but the choice is crucially important in determining the rate of convergence to the stationary distribution. We took  $q(\vec{x}|\vec{y})$  to be a multivariate Gaussian with covariance matrix given by the inverse of the FIM. In addition to the source parameters we included two additional parameters,  $k_A$  and  $k_E$ , that describe the noise levels in the A and E data channels:

$$\begin{aligned} S_n^A(f) &= k_A S_n(f) \\ S_n^E(f) &= k_E S_n(f). \end{aligned} \quad (23)$$

In a given realization of the instrument noise  $k_A$  and  $k_E$  will differ from unity by some random amount  $\delta$ . The quantity  $\delta$  will have a Gaussian distribution with variance  $\sigma^2 = 1/N$ , where  $N$  is the number of frequency bins being analyzed. The likelihood  $p(s|\vec{\lambda})$  can then be written as

$$p(s|\vec{\lambda}) = C' \exp \left[ -\frac{1}{2} (s - h | s - h) - N \ln(k_A k_E) \right] \quad (24)$$

where the constant  $C'$  is independent of the signal parameters  $\vec{\lambda}$  and the noise parameters  $k_A$  and  $k_E$ . We explored

the noise level estimation capabilities of our MCMC algorithm by starting  $k_A$  and  $k_E$  far from unity. As can be seen in Figure 2 the chain quickly identified the correct noise level.

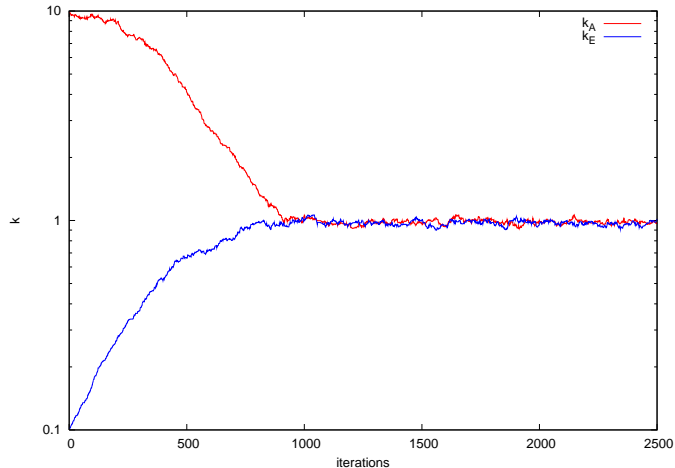


FIG. 2: Demonstration of the MCMC algorithm’s rapid determination of the injected noise level. The parameters  $k_A$  and  $k_E$  were initialized at 10 and 0.1 respectively.

#### IV. COMPARISON OF TECHNIQUES

We compared the Bayes Factor estimates obtained using the various methods in two ways. First, we fixed the frequency derivative of the source at  $q = 1$  and varied the SNR between 5 and 20 in unit increments. Second, we fixed the signal to noise ratio at  $\text{SNR} = 12$  and varied the frequency derivative of the source.

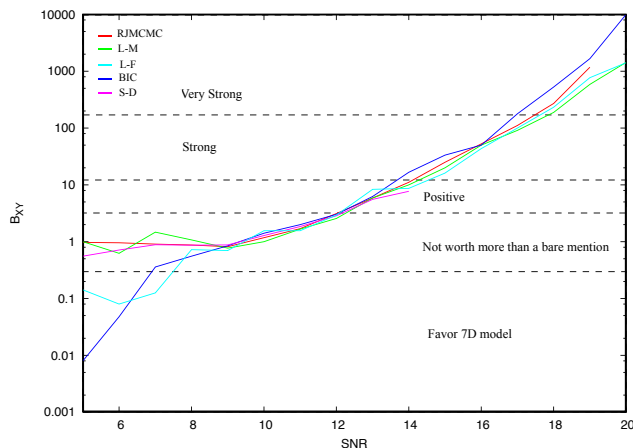


FIG. 3: Plot of the Bayes Factor estimates as a function of SNR for each of the approximation schemes described in the text.

The results of the first test are shown in Figure 3. We see that all five methods agree very well for  $\text{SNR} > 7$ .

As expected, the Laplace-Metropolis and Savage-Dicke methods provide the best approximation to the “Gold Standard” RJMCMC estimate, showing good agreement all the way down to  $\text{SNR} = 5$ . Most importantly, all five methods agree on when the 8-dimensional source model is favored over the 7-dimensional model, placing the transition point at  $\text{SNR} \simeq 12.2$ . To get a rough estimate for the numerical error in the various Bayes Factor estimates we repeated the  $\text{SNR} = 15$  case 10 times using different random number seeds. We found that the numerical error was enough to account for any quantitative differences between the estimates returned by the various approaches.

It is interesting to compare the Bayesian model selection results to the frequentist “3- $\sigma$ ” rule for positive detection:

$$|\bar{q}| > 3\sigma_q, \quad (25)$$

where  $\bar{q}$  is the MAP estimate for the frequency change and  $\sigma_q$  is the standard deviation in  $q$  as determined by the FIM. For the source under consideration we found the “3- $\sigma$ ” rule to require  $\text{SNR} \simeq 13$  for a detection, in good agreement with the Bayesian analysis. This lends support to Seto’s [21] earlier FIM based study of the detectability of the frequency evolution of galactic binaries, but we should caution that the literature is replete with examples where the “3- $\sigma$ ” rule yields results in disagreement with Bayesian model selection and common sense [22].

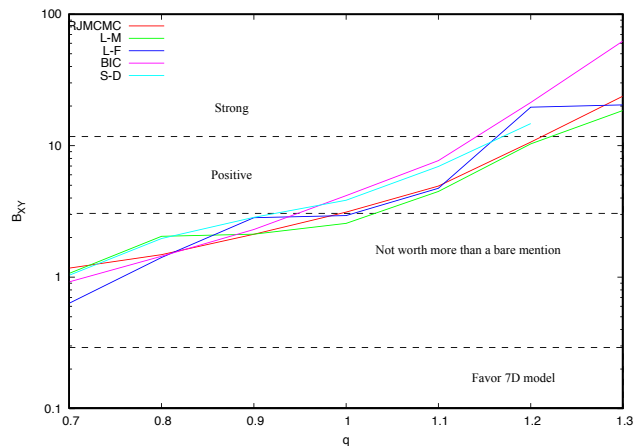


FIG. 4: Plot of the Bayes Factor estimates as a function of  $q$  for each of the approximation schemes described in the text. The signal to noise ratio was held fixed at  $\text{SNR} = 12$ .

The results of the second test are displayed in Figure 4. In this case all five methods produced results that agree to within numerical error.

While the results shown here are for a particular choice of source parameters, we found similar results for other sets of source parameters. In general all five methods for estimating the Bayes Factor gave consistent results for signals with  $\text{SNR} > 7$ . One exception to this general

trend were sources with inclinations close to zero, as then the PDFs tend to be highly non-gaussian. The Laplace-Metropolis and Laplace-Fisher approximations suffered the most in those cases.

## V. ASTROPHYSICAL PRIORS

Astrophysical considerations lead to very strong priors for the frequency evolution of galactic binaries. The detached systems, which are expected to account for the majority of LISA sources, will evolve under gravitational radiation reaction in accord with the leading order quadrupole formula:

$$\dot{f} = \frac{3(8\pi)^{8/3}}{40} f^{11/3} \mathcal{M}^{5/3}, \quad (26)$$

where  $\mathcal{M}$  is the chirp mass. Contact binaries undergoing stable mass transfer from the lighter to the heavier component are driven to longer orbital periods by angular momentum conservation. The competition between the effects of mass transfer and gravitational wave emission lead to a formula for  $\dot{f}$  with the same frequency and mass scaling as (26), but with the opposite sign and a slightly lower magnitude [23].

Population synthesis models, calibrated against observational data, yield predictions for the distribution of chirp masses  $\mathcal{M}$  as a function of orbital frequency. These distributions can be converted into priors on  $q$ . In constructing such priors one should also fold in observational selection effects, which will favor systems with larger chirp mass (the GW amplitude scales as  $\mathcal{M}^{5/6}$ ). To get some sense of how such priors will affect the model selection we took the chirp mass distribution for detached systems at  $f \sim 5$  mHz from the population synthesis model described in Ref. [24], (kindly provided to us by Gijs Nelemans), and used (26) to construct the prior on  $q$  shown in Figures 5 and 6 (observation selection effects were ignored). The prior has been modified slightly to give a small but non-vanishing weight to sources with  $q = 0$ . The astrophysically motivated prior has a very sharp peak at  $q = 0.64$ , and we use this value when fixing the frequency derivative for the 7-dimensional model.

To explore the impact on model selection when such a strong prior has been adopted we simulated a source with  $q = 1$  and varied the SNR. The RJMCMC algorithm was applied using chains of length  $10^7$  in conjunction with a fixed 8-dimensional MCMC (also allowed to run for  $10^7$  iterations) in order to compare the RJMCMC results with the Savage-Dickie density ratio.

The results of this first exploration are shown in Figure 5. We found that for  $\text{SNR} < 15$  the marginalized PDF very closely resembled the prior distribution. This demonstrates that the information content of the data is insufficient to change our prior belief about the value of the frequency derivative. As the SNR increased, however, the PDF began to move away from the prior until we reached  $\text{SNR}=30$  when the astrophysical prior had a

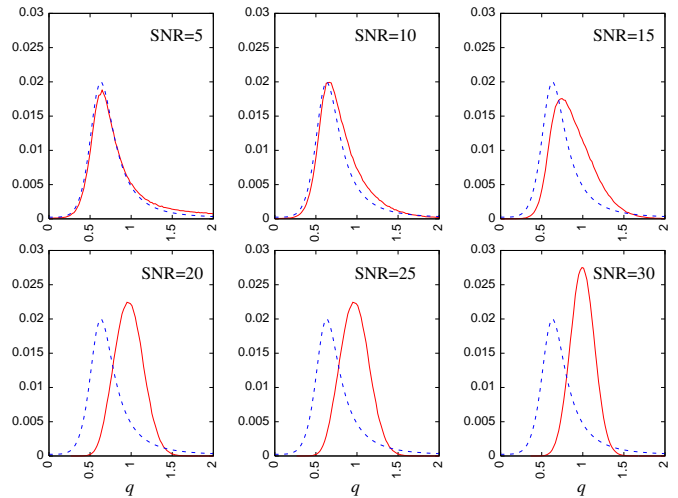


FIG. 5: Comparison between astrophysically motivated prior distribution of  $q$  for  $f = 5$  mHz and  $T_{\text{obs}} = 2$  years (dashed, blue) to marginalized PDF (solid, red) for sources injected with  $q = 1$  and SNRs varying from 5 to 30.

SNR	$B_{XY}$ (SD)	$B_{XY}$ (RJMCMC)
5	0.926	1.015
10	0.977	0.996
15	0.749	0.742
20	0.427	0.427
25	0.176	0.177
30	0.060	0.056

TABLE III: Savage-Dickie density ratio estimates of  $B_{XY}$  for sources with  $q = 1$  and SNRs varying from 5 to 30. Comparisons with RJMCMC explorations of the same data set show excellent agreement between the two methods.

negligible effect on the shape of the posterior, signaling confidence in the quoted measurement of  $q$ . This qualitative assessment of model preference is strongly supported by the Bayes factor estimation made by the RJMCMC algorithm as can be seen in Table III. It should also be noted that the excellent agreement between the RJMCMC and S-D estimates for Bayes factor  $B_{XY}$ . Both methods indicate that for the chosen value of  $q = 1$ , the signal-to-noise needs to exceed  $\text{SNR} \sim 25$  for the 8-dimensional model to be favored. This is in contrast to the case discussed earlier where a uniform prior was adopted for the frequency derivative, and the model selection methods began showing a preference for the 8-dimensional model around  $\text{SNR}=12$ .

Figure 6 shows the impact of the astrophysically motivated prior when the SNR was held at 15 and four different injected values for  $q$  were adopted, corresponding to the full width at half maximum (FWHM) and full width at quarter maximum (FWQM) of the prior distribution. The Bayes factors listed in Table IV indicate that for modestly loud sources with  $\text{SNR}=15$  the model selection techniques do not favor updating our estimate of the fre-



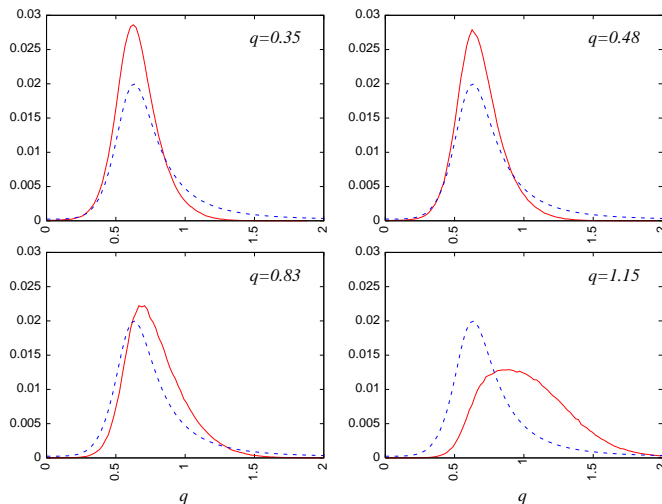


FIG. 6: Marginalized PDF (solid, red) for fixed SNR=15 injected sources with  $q$  corresponding to FWHM and FWQM of the astrophysical prior (dashed, blue)

$q$	$B_{XY}$ (SD)	$B_{XY}$ (RJCMC)
0.35	1.412	1.414
0.48	1.381	1.388
0.83	1.059	1.052
1.15	0.432	0.428

TABLE IV: Savage-Dickie and RJCMC density ratio estimates of  $B_{XY}$  for sources with SNR=15 and  $q$  at FWHM and FWQM of astrophysical prior

quency derivative until the frequency derivative exceeds  $q = 1.2$ .

## VI. DISCUSSION

We have found that the several common methods for estimating Bayes Factors give good agreement when applied to the the model selection problem of deciding when the data from the LISA observatory can be used to detect the orbital evolution of a galactic binary. The methods studied require varying degrees of effort to implement and calculate, and although found to be accurate in this test case, it is clear that some of these methods would be inappropriate approximations for more physically relevant examples.

If a RJCMC algorithm is used as the sole model selection technique, the resistance of the algorithm to change dimension, especially when making multi-dimensional jumps, can result in invalid model selection unless the chains are run for a very large numbers of steps. In the examples we studied the transdimensional jumps only had to span one dimension, and our basic RJCMC algorithm performed well. However, a more sophisticated implementation, using *e.g.* rejection sampling or coupled chains, will be required to select the

number of sources, as this requires jumps that span seven or more dimensions.

The Laplace-Metropolis method for approximating the model evidence is more robust than the commonly used Fisher Information Matrix approximation of the Hessian of the PDF. Implementing an LM evidence estimation is a somewhat costly because of the need to fit the posterior to a minimum volume ellipsoid.

The Savage-Dickie approximation is more economical than the RJCMC or LM methods, but is limited by the requirement that the competing models *must* be nested.

The Bayes Information Criterion approximation to the evidence is by far the cheapest to implement, and is able to produce reliable results when the SNR is high. It has therefore shown the most promise as an ‘on the fly’ model determination scheme. More thorough (and therefore more costly) methods such as RJCMC and LM could then be used to refine the conclusions initially made by the BIC.

Our investigation using a strong astrophysical prior indicated that the gravitational wave signals will need to have high signal-to-noise (SNR > 25), or moderate signal-to-noise (SNR > 15) and frequency derivatives far from the peak of the astrophysical distribution, in order to update our prior belief in the value of the frequency derivative. In other words, the frequency derivative will only been needed as a search parameter for a small number of bright high frequency sources.

## Acknowledgments

This work was supported by NASA Grant NNG05GI69G. We are most grateful to Gijs Nelemans for providing us with data from his population synthesis studies.

## Appendix A

To leading order in the eccentricity,  $e$ , the Cartesian coordinates of the  $i^{\text{th}}$  LISA spacecraft are given by [25]

$$\begin{aligned}
 x_i(t) &= R \cos(\alpha) + \frac{1}{2}eR \left( \cos(2\alpha - \beta_i) - 3 \cos(\beta) \right) \\
 y_i(t) &= R \sin(\alpha) + \frac{1}{2}eR \left( \sin(2\alpha - \beta_i) - 3 \sin(\beta) \right) \\
 z_i(t) &= -\sqrt{3}eR \cos(\alpha - \beta_i).
 \end{aligned} \tag{27}$$

In the above  $R = 1$  AU, is the radial distance of the guiding center,  $\alpha = 2\pi f_m t + \kappa$  is the orbital phase of the guiding center, and  $\beta_i = 2\pi(i - 1)/3 + \lambda$  ( $i = 1, 2, 3$ ) is the relative phase of the spacecraft within the constellation. The parameters  $\kappa$  and  $\lambda$  give the initial ecliptic longitude and orientation of the constellation. The distance between the spacecraft is  $L = 2\sqrt{3}eR$ . Setting  $e = 0.00985$  yields  $L = 5 \times 10^9$  m.



An arbitrary gravitational wave traveling in the  $\hat{k}$  direction can be written as the linear sum of two independent polarization states

$$\mathbf{h}(\xi) = h_+(\xi)\varepsilon^+ + h_\times(\xi)\varepsilon^\times \quad (28)$$

where the wave variable  $\xi = t - \hat{k} \cdot \mathbf{x}$  gives the surfaces of constant phase. The polarization tensors can be expanded in terms of the basis tensors  $\mathbf{e}^+$  and  $\mathbf{e}^\times$  as

$$\begin{aligned} \varepsilon^+ &= \cos(2\psi)\mathbf{e}^+ - \sin(2\psi)\mathbf{e}^\times \\ \varepsilon^\times &= \sin(2\psi)\mathbf{e}^+ + \cos(2\psi)\mathbf{e}^\times, \end{aligned} \quad (29)$$

where  $\psi$  is the polarization angle and

$$\begin{aligned} \mathbf{e}^+ &= \hat{u} \otimes \hat{u} - \hat{v} \otimes \hat{v} \\ \mathbf{e}^\times &= \hat{u} \otimes \hat{v} + \hat{v} \otimes \hat{u}. \end{aligned} \quad (30)$$

The vectors  $(\hat{u}, \hat{v}, \hat{k})$  form an orthonormal triad which may be expressed as a function of the source location on the celestial sphere

$$\begin{aligned} \hat{u} &= \cos\theta \cos\phi \hat{x} + \cos\theta \sin\phi \hat{y} - \sin\theta \hat{z} \\ \hat{v} &= \sin\phi \hat{x} - \cos\phi \hat{y} \\ \hat{k} &= -\sin\theta \cos\phi \hat{x} - \sin\theta \sin\phi \hat{y} - \cos\theta \hat{z}. \end{aligned} \quad (31)$$

For mildly chirping binary sources we have

$$\mathbf{h}(\xi) = \Re \left[ \left( A_+ \varepsilon^+ + e^{i3\pi/2} A_\times \varepsilon^\times \right) e^{i\Psi(\xi)} \right] \quad (32)$$

where

$$\begin{aligned} A_+ &= \frac{2\mathcal{M}(\pi f)^{2/3}}{D_L} (1 + \cos^2\iota) \\ A_\times &= -\frac{4\mathcal{M}(\pi f)^{2/3}}{D_L} \cos\iota. \end{aligned} \quad (33)$$

Here  $\mathcal{M}$  is the chirp mass,  $D_L$  is the luminosity distance and  $\iota$  is the inclination of the binary to the line of sight. Higher post-Newtonian corrections, eccentricity of the orbit, and spin effects will introduce additional harmonics. For chirping sources the adiabatic approximation requires that the frequency evolution  $\dot{f}$  occurs on a timescale long compared to the light travel time in the interferometer:  $f/\dot{f} \ll L$ . The gravitational wave phase can be approximated as

$$\Psi(\xi) = 2\pi f_0 \xi + \pi \dot{f}_0 \xi^2 + \varphi_0, \quad (34)$$

where  $\varphi_0$  is the initial phase. The instantaneous frequency is given by  $2\pi f = \partial_t \Psi$ :

$$f = (f_0 + \dot{f}_0 \xi)(1 - \hat{k} \cdot \mathbf{v}). \quad (35)$$

The general expression for the path length variation caused by a gravitational wave involves an integral in  $\xi$  from  $\xi_i$  to  $\xi_f$ . Writing  $\xi = \xi_i + \delta\xi$  we have

$$\Psi(\xi) \simeq 2\pi(f_0 + \dot{f}_0 \xi_i) \delta\xi + \text{const.} \quad (36)$$

Thus, we can treat the wave as having fixed frequency  $f_0 + \dot{f}_0 \xi_i$  for the purposes of the integration, and then increment the frequency forward in time in the final expression [26]. The path length variation is then given by [25, 26]

$$\delta\ell_{ij}(\xi) = L \Re \left[ \mathbf{d}(f, t, \hat{k}) : \mathbf{h}(\xi) \right], \quad (37)$$

where  $\mathbf{a} : \mathbf{b} = a^{ij} b_{ij}$ . The one-arm detector tensor is given by

$$\mathbf{d}(f, t, \hat{k}) = \frac{1}{2} \left( \hat{r}_{ij}(t) \otimes \hat{r}_{ij}(t) \right) \mathcal{T}(f, t, \hat{k}), \quad (38)$$

and the transfer function is

$$\begin{aligned} \mathcal{T}(f, t, \hat{k}) &= \text{sinc} \left( \frac{f}{2f_*} \left( 1 - \hat{k} \cdot \hat{r}_{ij}(t) \right) \right) \\ &\times \exp \left( i \frac{f}{2f_*} \left( 1 - \hat{k} \cdot \hat{r}_{ij}(t) \right) \right), \end{aligned} \quad (39)$$

where  $f_* = 1/(2\pi L)$  is the transfer frequency and  $f = f_0 + \dot{f}_0 \xi$ . The expression can be attacked in pieces. It is useful to define the quantities

$$d_{ij}^+(t) \equiv (\hat{r}_{ij}(t) \otimes \hat{r}_{ij}(t)) : \mathbf{e}^+ \quad (40)$$

$$d_{ij}^\times(t) \equiv (\hat{r}_{ij}(t) \otimes \hat{r}_{ij}(t)) : \mathbf{e}^\times. \quad (41)$$

and  $y_{ij}(t) = \delta\ell_{ij}(t)/(2L)$ . Then

$$y_{ij}(t) = \Re \left[ y_{ij}^{\text{slow}}(t) e^{2\pi i f_0 t} \right], \quad (42)$$

where

$$\begin{aligned} y_{ij}^{\text{slow}}(t) &= \frac{\mathcal{T}(f, t, \hat{k})}{4} \left( (d_{ij}^+(t)(A_+(t) \cos(2\psi)) \right. \\ &\quad \left. + e^{3\pi i/2} A_\times(t) \sin(2\psi)) \right. \\ &\quad \left. + d_{ij}^\times(t)(e^{3\pi i/2} A_\times(t) \cos(2\psi) \right. \\ &\quad \left. - A_+(t) \sin(2\psi)) \right) e^{(\pi i \dot{f}_0 \xi^2 + i\varphi_0 - 2\pi i f_0 \hat{k} \cdot \mathbf{x})} \end{aligned} \quad (43)$$

It is a simple exercise to derive explicit expressions for the antenna functions and the transfer function appearing in  $y_{ij}^{\text{slow}}(t)$  using (27) and (31).

In the Fourier domain the response can be written as

$$y_{ij}(t) = \Re \left[ \left( \sum_n a_n e^{2\pi i n t / T_{\text{obs}}} \right) e^{2\pi i f_0 t} \right], \quad (44)$$

where the coefficients  $a_n$  can be found by a numerical FFT of the slow terms  $y_{ij}^{\text{slow}}(t)$ . Note that the sum over  $n$  should extend over both negative and positive values. The number of time samples needed in the FFT will depend on  $f_0$  and  $\dot{f}_0$  and  $T_{\text{obs}}$ , but is less than  $2^9 = 512$  for any galactic sources we are likely to encounter when  $T_{\text{obs}} \leq 2\text{yr}$ . The bandwidth of a source can be estimated as

$$B = 2(4 + 2\pi f_0 R \sin(\theta)) f_m + \dot{f}_0 T_{\text{obs}}. \quad (45)$$

The number of samples should exceed  $2BT_{\text{obs}}$ . The Fourier transform of the fast term can be done analytically:

$$e^{2\pi if_0 t} = \sum_m b_m e^{2\pi imt/T_{\text{obs}}} \quad (46)$$

where

$$b_m = T_{\text{obs}} \text{sinc}(x_m) e^{ix_m} \quad (47)$$

and

$$x_m = f_0 T_{\text{obs}} - m. \quad (48)$$

The cardinal sine function in (46) ensures that the Fourier components  $b_m$  away from resonance,  $x_m \approx 0$ , are quite small. It is only necessary to keep  $\sim 100 \rightarrow 1000$  terms either side of  $p = [f_0 T_{\text{obs}}]$ , depending on how bright the source is, and how far  $f_0 T_{\text{obs}}$  is from an integer. We now have

$$y_{ij}(t) = \Re \left[ \left( \sum_j c_j e^{2\pi ijt/T_{\text{obs}}} \right) \right], \quad (49)$$

where

$$c_j = \sum_n a_n b_{j-n}. \quad (50)$$

The final step is to ensure that our Fourier transform yields a real  $y_{ij}(t)$ . This is done by setting the final answer for the Fourier coefficients equal to  $d_j = (c_j + c_{-j}^*)/2$ .

But since  $x_m$  never hits resonance for positive  $j$  (we are not interested in the negative frequency components  $j < 0$ ), we can neglect the second term and simply write  $d_j = c_j/2$ .

Basically what we are doing is hetrodyning the signal to the base frequency  $f_0$ , then Fourier transforming the slowly evolving hetrodyned signal numerically. We then convolve these Fourier coefficients with the analytically derived Fourier coefficients of the carrier wave.

The Michelson type TDI variables are given by

$$X(t) = y_{12}(t - 3L) - y_{13}(t - 3L) + y_{21}(t - 2L) - y_{31}(t - 2L) + y_{13}(t - L) - y_{12}(t - L) + y_{31}(t) - y_{21}(t), \quad (51)$$

$$Y(t) = y_{23}(t - 3L) - y_{21}(t - 3L) + y_{32}(t - 2L) - y_{12}(t - 2L) + y_{21}(t - L) - y_{23}(t - L) + y_{12}(t) - y_{32}(t), \quad (52)$$

$$Z(t) = y_{31}(t - 3L) - y_{32}(t - 3L) + y_{13}(t - 2L) - y_{23}(t - 2L) + y_{32}(t - L) - y_{31}(t - L) + y_{23}(t) - y_{13}(t). \quad (53)$$

Note that in the Fourier domain

$$X(f) = \tilde{y}_{12}(f) e^{-3if/f^*} - \tilde{y}_{13}(f) e^{-3if/f^*} + \tilde{y}_{21}(f) e^{-2if/f^*} - \tilde{y}_{31}(f) e^{-2if/f^*} + \tilde{y}_{13}(f) e^{-if/f^*} - \tilde{y}_{12}(f) e^{-if/f^*} + \tilde{y}_{31}(f) - \tilde{y}_{21}(f). \quad (54)$$

This saves us from having to interpolate in the time domain. We just combine phase shifted versions of our original Fourier transforms.

- 
- [1] Raftery, A.E., *Practical Markov Chain Monte Carlo*, (Chapman and Hall, London, 1996).
- [2] Trotta, R., astro-ph/0504022 (2005).
- [3] Sambridge, M., Gallagher, K., Jackson, A. & Rickwood, P., *Geophys. J. Int.* **167** 528-542 (2006).
- [4] Bender, P. *et al.*, *LISA Pre-Phase A Report*, (1998).
- [5] S. Timpano, L. J. Rubbo & N. J. Cornish, *Phys. Rev. D* **73** 122001 (2006).
- [6] Cornish, N.J. & Crowder, J., *Phys. Rev. D* **72**, 043005 (2005).
- [7] C. Andrieu & A. Doucet, *IEEE Trans. Signal Process.* **47** 2667 (1999).
- [8] R. Umstatter, N. Christensen, M. Hendry, R. Meyer, V. Simha, J. Veitch, S. Vieglund & G. Woan, gr-qc/0503121 (2005).
- [9] J. Crowder & N. J. Cornish, *Phys. Rev. D* **75** 043008 (2007).
- [10] T. A. Prince, M. Tinto, S. L. Larson & J. W. Armstrong, *Phys. Rev. D* **66**, 122002 (2002).
- [11] Gamerman, D., *Markov Chain Monte Carlo: Stochastic Simulation of Bayesian Inference*, (Chapman & Hall, London, 1997).
- [12] Metropolis, N., Rosenbluth, A.W., Rosenbluth, M.N., Teller, A.H., & Teller E., *J. Chem. Phys.* **21**, 1087 (1953).
- [13] Hastings, W.K., *Biometrika* **57**, 97 (1970).
- [14] Jeffreys, H. *Theory of Probability*, Third Edition. (Oxford University Press 1961).
- [15] Green, P.J., *Biometrika* **82** 711-32 (1995).
- [16] Lopes, H.F., & West M., *Statistica Sinica* **14**, 41-67 (2004).
- [17] Kim van der Linde (2004) MVE: Minimum Volume Ellipsoid estimation for robust outlier detection in multivariate space, Java version. Website: <http://www.kimvdlinde.com/professional/mve.html>.
- [18] Dickey, J.M., *Ann. Math. Stat.*, **42**, 204 (1971).
- [19] Schwarz, G., *Ann. Stats.* **5**, 461 (1978).
- [20] K. Arnaud *et al.*, preprint gr-qc/0701170 (2007).
- [21] Seto, N., *Mon. Not. Roy. Astron. Soc.* **333**, 469-474 (2002).
- [22] D. Lindley, *Biometrika* **44** 187 (1957).
- [23] G. Nelemans, L. R. Yungelson & S. F. Portegies Zwart, *Mon. Not. Roy. Astron. Soc.* **349** 181, (2004).
- [24] G. Nelemans, L. R. Yungelson & S. F. Portegies Zwart, *A&A* **375**, 890 (2001).
- [25] Cornish, N.J. & Rubbo, L.J., *Phys. Rev. D* **67**, 022001 (2003).
- [26] Cornish, N.J., Rubbo, L.J. & Poujade, O., *Phys. Rev. D* **69**, 082003 (2004).

[27] While this count is only strictly correct for point-like masses, frequency evolution due to tides and mass transfer can also be described by the same two parameters for

the majority of sources in the LISA band.